Ab initio total-energy pseudopotential calculations for polymorphic B₂O₃ crystals

Akira Takada

Fundamental Research Laboratory, Asahi Glass Co., Ltd., 1150 Hazawa-cho, Yokohama 221, Japan

C. R. A. Catlow and J. S. Lin

Davy Faraday Research Laboratory, Royal Institution of Great Britain, 21 Albermarle Street, London W1X 4BS, United Kingdom

G. D. Price

Research School of Geological and Geophysical Sciences, Birkbeck College and University College London, Gower Street, London W1E 6BT, United Kingdom

M. H. Lee, V. Milman, and M. C. Payne Cavendish Laboratory, Madingley Road, Cambridge, CB3 OHE, United Kingdom (Received 12 July 1994)

We use *ab initio* pseudopotential electronic-structure methods to describe successfully both the detailed static structures and the structural transformation in B_2O_3 crystals. Employing a reduced cell volume, with full relaxation of all internal coordinates, our calculations model the structural transformation from the polymorph containing the BO_3 triangular unit into that containing the BO_4 tetrahedral unit. In order to interpret the mechanism, individual energy contributions to the total energy are analyzed.

I. INTRODUCTION

 B_2O_3 is an interesting material, showing two polymorphs in which the boron atoms have different coordination numbers (see Figs. 1 and 2). Neither form of crystalline trioxide occurs naturally. Furthermore, it is not easy even under special conditions to prepare crystals and measure their properties. In such cases computer simulations can play an important role in determining the structural and physical properties. Advances in the techniques of electronic-structure calculations make it possible to calculate total energies with high accuracy. These computer simulation techniques are currently used to

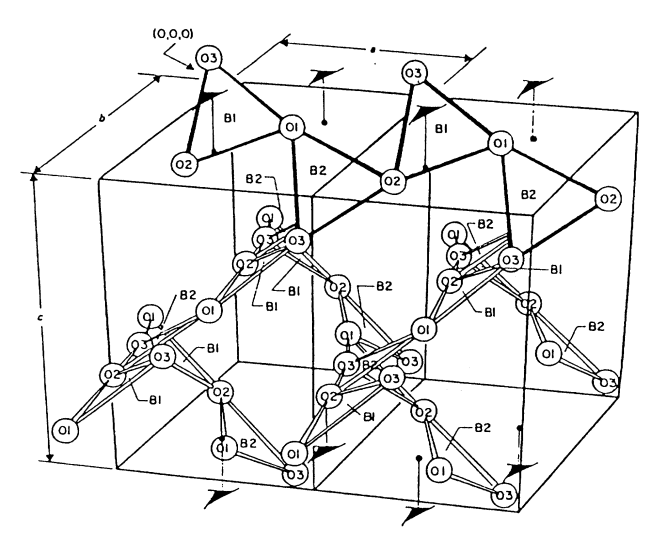


FIG. 1. The B_2O_3 -I structure (Ref. 15).

study not only static but also dynamical structures in both the crystalline and amorphous states, although there are still considerable limitations on the size of a system that can be studied (in particular, the number of independent atoms in the unit cell) because of the constraints imposed by computer resources.

In a companion study¹ of B₂O₃ and borates using periodic *ab initio* Hartree-Fock techniques, we provide a consistent interpretation of the structure and bonding of borates which accords well with empirical concepts regarding the structure and bonding in these crystals. However, these methods were unable to study fully relaxed structures in detail, as automatic relaxation of cell dimensions or internal coordinates is not available in the present version of the periodic *ab initio* Hartree-Fock program (CRYSTAL92).

In this paper we discuss how the structures and bulk

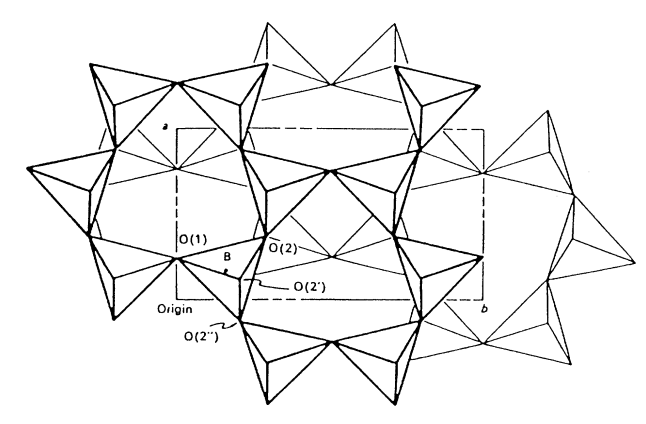


FIG. 2. The B₂O₃-II structure (Ref. 16).

moduli of B_2O_3 crystals have been determined employing the local-density formalism (LDF) electronic-structure methods rather than Hartree-Fock techniques. Our studies used the code CASTEP, which performs total-energy pseudopotential calculation. CASTEP has two distinctive features: first, the internal coordinates can be automatically relaxed so that the structure with the minimum total energy is obtained; second, it has the option of *ab initio* molecular-dynamics simulation, although this was not employed in the present case.

The next section examines the theoretical techniques in more detail and explains the contrast between the theoretical approaches adopted in this paper compared with the quantum-chemical, Hartree-Fock methods. We then apply the LDF technique to optimize the lattice parameters and internal coordinates of B_2O_3 . After the optimized structures of both phases have been identified, the total energies of several points with different cell volumes were calculated and bulk moduli were estimated. Finally, we use the results of these calculations to provide the first suggestion of a mechanism for the structural transformation between B_2O_3 polymorphs.

II. THEORETICAL METHOD

CASTEP is a powerful code for calculating the quantum-mechanical total energy of a structure and then minimizing it with respect to its electronic and nuclear coordinates. When compared with the Hartree-Fock based quantum-chemical methods, there are three distinctly different approaches involved in the techniques used by CASTEP:

(i) Density-functional theory⁴ and the local-density approximation (LDA) (Ref. 5) are employed to model the electron-electron interactions. The difference in formulation between Hartree-Fock (HF) theory and density functional theory (DFT) can be summarized as follows:⁶ DFT,

$$E = E[\rho, R], \tag{1}$$

$$E = T[\rho] + U[\rho] + E_{xc}[\rho] , \qquad (2)$$

$$\rho(r) = \sum_{occ} |\Psi_i(r)|^2 , \qquad (3)$$

$$\partial E/\partial \rho = 0$$
, (4)

$$[-1/2\nabla^2 + V_c(r) + \mu_{xc}(r)]\Psi_i = \varepsilon_i \Psi_i. \tag{5}$$

HF,

$$E = E[\Psi, R], \tag{6}$$

$$E = \int \Psi^* [\Sigma_i h_i + \Sigma_{i>i} 1/r_{ii}] \Psi \delta \tau , \qquad (7)$$

$$\Psi = |\Psi(1), \Psi(2), \dots, \Psi(n)|, \qquad (8)$$

$$\partial E/\partial \Psi = 0$$
, (9)

$$[-1/2\nabla^2 + V_c(r) + \mu_r^i(r)]\Psi_i = \varepsilon_i \Psi_i , \qquad (10)$$

where E is total energy, Ψ is wave function, ρ is electron density, R or r is coordinate for nucleus or electron, h is the Hamiltonian, T is kinetic energy, U is electrostatic or Coulomb energy term, μ_{xc} or μ_x is a many-body term or

exchange term, and ε is the eigenvalue.

The biggest difference between the two theories is in the term μ_{xc} or μ_x . In HF theory the exchange term μ_x only describes exchange effects and is calculated from all the wave functions based on the orbitals

$$\begin{split} \mu_{x}^{i}(r) &= -\sum_{j} \delta(\sigma_{i}, \sigma_{j}) \\ &\times \frac{\int \Psi_{i}^{*}(r) \Psi_{j}^{*}(r') (1/|r-r'|) \Psi_{j}(r) \Psi_{i}(r') dr'}{\Psi_{i}^{*}(r) \Psi_{i}(r)} \end{split} \tag{11}$$

where σ is the spin.

On the other hand, in DFT theory μ_{xc} contains all the many-body effects and it is calculated from the total electron density

$$\mu_{\rm xc}(r) = \delta E_{\rm xc}[\rho]/d\rho(r) \ . \tag{12}$$

Further, LDA provides a good approximation,

$$E_{\rm xc}[\rho] \approx \int \rho(r) \varepsilon_{\rm xc}[\rho(r)] dr$$
 , (13)

where $\varepsilon_{xc}[\rho]$ is the exchange-correlation energy per electron in an interacting electron system of constant density ρ , and

$$\mu_{xc}(r) = \varepsilon_{xc}[\rho(r)] + \rho(r) \{\delta E_{xc}[\rho(r)]/d\rho(r)\}. \tag{14}$$

This approximation is generally known to yield only a small percentage error both in the total energy and in the structural parameters. However, cohesive energies can be in error by more than 10%.

(ii) Pseudopotential theory^{7,8} is used to model the electron-ion interactions. The strong electron-nuclear potential is replaced by a much weaker pseudopotential, and plane waves are used as basis functions to model the electron density outside the core region. This pseudopotential technique makes the solution of Schrödinger's equations much simpler. The important point is that the selection of the pseudopotential is as crucial as the selection of the basis set in the quantum-chemical calculation. Lin et al.9 have developed an efficient and general procedure to generate optimized and transferable nonlocal separable ab initio pseudopotentials. Another point is that the cutoff energy, i.e., the number of plane waves, has to be so large that the total energy is converged. For oxides a larger number of plane waves are necessary than for semiconductors, to express the more complex charge-density distribution.

(iii) The counterpart to the self-consistent field method in the quantum-chemical terms is the use of the conjugate-gradients technique, i.e., iterative diagonalization approaches, $^{3,10-12}$ are employed to relax the electronic coordinates. This provides an efficient method to minimize the Kohn-Sham energy functional for large systems and it is applicable to oxide materials.

III. STRUCTURAL SIMULATION FROM FIRST PRINCIPLES

A. Selection of model

The pseudopotentials for boron and oxygen were generated using Lin's scheme.⁹ For both crystal structures

TABLE I. Relation between cell volume and calculated total energy in B_2O_3 -I and B_2O_3 -II.

$\mathbf{B}_{2}\mathbf{O}_{3}$ -I $(v/v_{0})^{1/3}$	Total energy (eV/B ₂ O ₃)
(0,00)	Total energy (evy byes)
1.005	-1442.840
1.0	-1442.892
0.995	-1442.925
0.990	-1442.964
0.985	-1442.969
0.980	-1442.977
0.975	— 1442.953
B ₂ O ₃ -II	
$(v/v_0)^{1/3}$	Total energy (eV/B ₂ O ₃)
1.0	—1443.124
0.99	-1443.221
0.98	— 1443.254
0.975	-1443.258
0.97	-1443.237

of B_2O_3 , the same cutoff energy of 500 eV for the plane-wave basis set was used to achieve a reasonable convergence of the total energy. The number of plane waves used was 3459 for the B_2O_3 -I system (15 atoms) and 1890 for B_2O_3 -II (10 atoms).

The other important factor is the k-point sampling. The Bloch theorem changes the problem of calculating an infinite number of electronic wave functions to calculating a finite number of electronic wave functions at an infinite number of k points. However, it is possible to represent the electronic wave functions over a region of kspace by the wave functions at a single k point. Several methods^{13,14} have been devised for obtaining an accurate approximation for the total energy with a very small number of k points. Generally speaking, the denser the set of k points sampled, the more accurate is the result. However, both the unit cells for B₂O₃ crystals are too large for the calculation with multi k points. Therefore, several single k points were investigated, and among them the single k point, which gives the smallest cell stress and internal force, was selected. The resulting kpoint was $(\frac{1}{3}, \frac{1}{3}, \frac{1}{4})$ for B_2O_3 -I and $(\frac{1}{4}, \frac{1}{4}, \frac{1}{4})$ for B_2O_3 -II. This difference results from the difference in crystal symmetry between the two polymorphs. 15,16

B. Optimization of structure

First, the relation between cell volume and total energy was calculated under the condition that the internal coordinates remained fixed (Table I). When the optimized structure (i.e., the structure with minimum total energy) is compared with experiment, the error in the lattice constant is -2.0% for B_2O_3 -I and -2.5% for B_2O_3 -II. The error in volume is converted into -5.9% for B_2O_3 -I and -7.3% for B_2O_3 -II. This result is satisfactory, considering that a common pseudopotential set for boron and oxygen was used for both polymorphs, and only one k point was sampled.

Second, internal coordinates were relaxed, with the constraint that the optimized cell parameters remain fixed. The initial and final (optimized) total energies, bond lengths, and angles are shown in Tables II and III.

Regarding the relative stability of the two polymorphs, the total energy of B₂O₃-II is lower than that of B₂O₃-I, regardless of whether the internal coordinates are re-Periodic Hartree-Fock calculations employing the CRYSTAL code also show the same result. However, the phase diagram of the B₂O₃ system¹⁷ suggests that B₂O₃-I is more stable than B₂O₃-II under ambient conditions. More sophisticated calculations may be required in order to reproduce the small difference in total energy in either method. Thus Nada et al. 18 showed that to reproduce correctly the relative energies of quartz and stishovite it was necessary to use high-quality basis sets in their CRYSTAL calculations. CASTEP calculations may need a more dense set of k point sampling to give the correct order of energies for the two phases of B₂O₃. We should also point out that the relative energies of the two phases are unknown and that the difference in free energy may include a large contribution from entropic factors.

When the calculated bond lengths and bond angles are compared with the experimental values, the errors in the bond lengths and bond angles are within 0.055 Å and 3.5°. Both calculated structures reproduce the corresponding experimental structures well. It is interesting to note the change of the B(1)-O(1) bond length in B₂O₃-II. In the CRYSTAL calculations the B(1)-O(1) bond is elongated by 10% with the constraint that all the other atomic positions are fixed. On the other hand, the B(1)-O(1) bond is shortened by 4% in the same manner as the other B-O bonds when all the atomic positioned are relaxed. Therefore, the full relaxation of internal coordinates is almost certainly important for discussing the detailed structure.

C. Estimation of bulk modulus

An estimate of the bulk modulus was obtained using the total-energy calculation technique. The procedure used was based on Murnaghan's equation.¹⁹ Several

TABLE II. Comparison of total energies between initial structures and final optimized structures in B_2O_3 -I and B_3O_3 -II.

	E1 (eV/B_2O_3) before relaxation	E2 (eV/ B_2O_3) after relaxation	E2-E1 (eV/B ₂ O ₃) difference	
B ₂ O ₃ -I	— 1442.977	-1443.059	-0.082	
$\mathbf{B_2O_3}$ -II	— 1443.258	-1443.358	-0.100	

TABLE III. Comparison of bond lengths and angles between experimental structures and final optimized structures in B₂O₃-I and B₂O₃-II.

	$\mathbf{B}_{2}\mathbf{C}$) ₃ -I		B_2C	₃ -II
Distances (Å)	Experiment ^a	Calculation		Experiment ^b	Calculation
B (1)- O (1)	1.404	1.354	B(1)-O(1)	1.373	1.358
-O(2)	1.366	1.329	-O(2)	1.507	1.461
-O (3)	1.336	1.338	-O(2')	1.506	1.451
B(2)-O(1)	1.336	1.329	-O(2'')	1.512	1.507
-O(2')	1.400	1.355	O(1)-O(2)	2.364	2.313
-O(3')	1.384	1.337	-O(2')	2.440	2.365
O(1)-O(2)	2.387	2.327	-O(2'')	2.409	2.408
	2.388	2.329	O(2)-O(2')	2.428	2.366
O(2)-O(3)	2.409	2.331	-O(2'')	2.394	2.351
	2.333	2.284	O(2')-O(2'')	2.389	2.350
O(3)-O(1)	2.309	2.285			
	2.409	2.343			
Angles (deg)					
O-B(1)-O	119.0	120.3	O-B(1)-O	110.2	110.2
	114.7	116.2		115.8	114.6
	126.2	122.8		113.1	113.7
O-B(2)-O	121.5	120.4		107.4	108.7
	124.6	123.0		104.9	104.3
	113.9	116.1		104.7	104.7
B-O(1)-B	130.5	131.2	B-O(1)-B	138.6	135.1
	128.3	131.2	-O (2)-	123.8	121.2
	133.3	133.5	-O(2')-	114.7	115.7
			-O(2")-	118.9	118.9

^aReference 15.

values for the total energy as a function of cell volume were fitted using least-square techniques to Murnaghan's equation;²⁰

$$E_{\text{tot}}(V) = B_0 V / B_0' [(V_0 / V)^{B_0'} / (B_0' - 1) + 1] + \text{const},$$
(15)

where B_0 and B_0 ' are the bulk modulus and its pressure derivative at the equilibrium volume V_0 ; both B_0 and B_0 ' were fitted

As each calculation of ionic relaxation requires a large amount of CPU time, only six points were calculated for both polymorphs. The cell volume was isotropically varied and then internal coordinates relaxed in each case. The relation between the cell volumes and the corresponding total energies is shown in Table IV. The calculated bulk moduli and the curve fitted to Murnaghan's equation are shown in Table V and Fig. 3. The estimated bulk modulus is 26 GPa for B_2O_3 -I and 126 GPa for B_2O_3 -II.

No experimental data of bulk modulus are available at present. The prediction of the bulk modulus is generally more difficult than that of lattice constants, and it is also very difficult to evaluate the error of these estimations.

TABLE IV. Relation between cell volume and total energy in B₂O₃-I and B₂O₃-II. (Each relative cell volume is the ratio to the corresponding optimized cell volume.)

	B_2O_3 -I		B_2O_3	-II
Volume ratio	Total energy (eV/B ₂ O ₃)	Difference	Total energy (eV/B ₂ O ₃)	Difference
0.6	-1440.68	+2.38	-1438.10	+5.26
0.8	-1442.44	+0.62	-1442.65	+0.71
1.0	-1443.06	± 0	-1443.36	± 0
1.1	-1442.99	+0.07	-1443.12	+0.24
1.2	-1442.75	+0.31	-1442.58	+0.78
1.3	-1442.36	+0.70	-1441.83	+1.53

^bReference 16.

TABLE V. Experimental density and calculated bulk moduli in B_2O_3 -I and B_2O_3 -II.

	B ₂ O ₃ -I ^a	B ₂ O ₃ -II ^b	Glass
Density (g/cm ³)	2.56	3.11	1.84-1.91
Bulk modulus			
(GPa)			
This work	26	126	
Empirical ^c	47	97	15
Experiment			15

^aReference 15.

For the CASTEP calculation, the cell volume is only varied isotropically; furthermore, a more dense set of k points would probably improve its accuracy. On the other hand, for the empirical equation detailed structural information is not taken into consideration.

D. Structural transformation

The nature of the ionic relaxation for different cell volumes can be used to study the transformation between the two structures. The optimized cell volume was changed by -40, -20, +10, +20, +30, +70, and

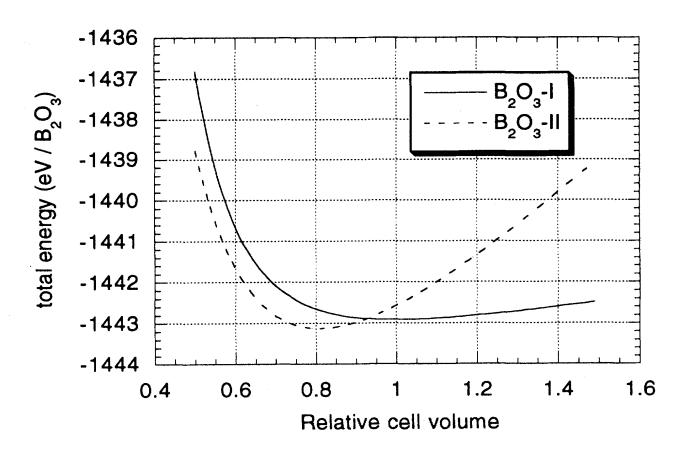


FIG. 3. Calculated "Murnaghan" curve for B_2O_3 -I and B_2O_3 -II. The relative cell volume is the ratio to the optimized B_2O_3 -I cell volume.

+100% for B_2O_3 -I and changed by -40, -20, +10, +20, and +30% for B_2O_3 -II. Their relaxed bond lengths and angles are summarized in Tables VI and VII. The structures calculated for B_2O_3 -I are discussed for three ranges of the cell volume as follows.

TABLE VI. Comparison of bond lengths and angles at different cell volumes in B_2O_3 -I. (Relative cell volume is the ratio to the optimized cell volume.)

Volume ratio		0.60	0.80	1.00	1.10	1.20	1.30	1.70	2.00
Lattice ratio		0.84	0.93	1.00	1.03	1.06	1.09	1.19	1.26
	exp.	_ cal.	cal.	cal.	cal.	cal.	cal.	cal.	cal.
Distance (Å)									
B(1)-O(1)	1.404	1.340	1.319	1.354	1.379	1.407	1.439	1.535	1.655
-O(2)	1.366	1.387	1.315	1.329	1.343	1.357	1.370	1.387	1.368
-O (3)	1.336	1.290	1.308	1.338	1.355	1.372	1.389	1.399	1.380
-O(2')	2.616	1.422	2.099	2.524	2.670	2.807	2.931		
B(2)-O(1)	1.336	1.338	1.314	1.329	1.344	1.358	1.371	1.390	1.368
-O(2')	1.400	1.340	1.320	1.355	1.379	1.407	1.440	1.542	1.656
-O(3')	1.384	1.289	1.305	1.337	1.354	1.371	1.388	1.398	1.379
-O(1")	2.636	1.423	2.119	2.529	2.675	2.812	2.935		
O(1)-O(2)	2.387	2.175	2.252	2.327	2.371	2.414	2.457	2.606	2.727
	2.388	2.176	2.254	2.329	2.372	2.417	2.460	2.618	2.727
O(2)-O(3)	2.409	2.271	2.332	2.331	2.346	2.414	2457	2.373	2.387
	2.333	2.034	2.184	2.284	2.337	2.388	2.439	2.503	2.503
O(3)-O(1)	2.309	2.030	2.184	2.285	2.339	2.372	2.441	2.504	2.502
	2.409	2.273	2.335	2.343	2.347	2.358	2.370	2.375	2.387
Angle (deg)									
O-B(1)-O	119.0	105.8	117.5	120.4	121.1	121.7	122.0	126.1	128.7
	114.7	101.1	112.5	116.2	117.7	118.6	119.4	117.0	110.7
	126.2	116.1	125.6	122.8	120.8	119.5	118.5	116.8	120.6
O-B(2)-O	121.5	105.8	117.7	120.4	121.2	121.8	122.2	126.4	128.6
	124.6	116.3	126.1	123.0	120.9	119.5	118.4	116.9	120.6
	113.9	101.3	112.6	116.3	117.6	118.5	119.2	116.7	110.8
B-O(1)-B	130.5	116.1	122.4	131.2	134.5	137.4	139.7	149.4	152.7
-O(2)-	128.3	116.3	122.4	131.2	134.5	137.2	139.1	149.2	152.8
-O(3)-	133.3	110.4	127.0	133.5	135.8	137.2	139.2	139.1	138.5

^bReference 16.

^cEmpirical equation between density (ρ) and bulk modulus (K) was employed. Reference 21. $\sqrt{(K/\rho)} = -1.75 + 2.36\rho$.

TABLE VII. Comparison of bond lengths and angles at different cell volumes in B₂O₃-II. (Relative cell volume is the ratio to the optimized cell volume.)

		0.60	0.80	1.00	1 10	1.20	1 20
Volume ratio		0.60	0.80	1.00	1.10		1.30
Lattice ratio		0.84		1.00	1.03	1.06	1.09
	exp.	cal.	cal.	cal.	cal.	cal.	cal.
Distance (Å)							
B(1)-O(1)	1.373	1.274	1.328	1.358	1.376	1.396	1.416
-O(2)	1.507	1.335	1.406	1.461	1.498	1.535	1.561
-O(2')	1.506	1.314	1.390	1.451	1.484	1.517	1.542
-O(2")	1.512	1.367	1.447	1.507	1.568	1.636	1.725
O(1)-O(2)	2.364	2.142	2.234	2.313	2.376	2.446	2.507
-O(2')	2.440	2.202	2.305	2.365	2.402	2.450	2.499
-O(2'')	2.409	2.205	2.319	2.408	2.464	2.530	2.604
O(2)-O(2')	2.428	2.125	2.257	2.366	2.428	2.489	2.539
-O(2'')	2.394	2.179	2.281	2.351	2.403	2.466	2.525
O(2')-O(2")	2.389	2.080	2.230	2.350	2.415	2.489	2.567
Angle (deg)							
O-B(1)-O	110.2	110.4	109.6	110.2	111.5	113.0	114.6
	115.8	116.6	115.9	114.6	114.2	114.5	115.3
	113.1	111.7	113.3	113.7	113.5	112.8	111.6
	107.4	106.7	107.6	108.7	109.0	107.7	109.9
	104.9	107.5	106.2	104.3	103.3	102.1	100.4
	104.7	101.8	103.6	104.7	104.6	104.2	103.5
B-O(1)-B	138.6	104.5	117.6	135.1	141.7	145.4	148.9
-O(2)-	123.8	112.1	117.0	121.2	121.5	121.8	119.4
-O(2')-	114.7	111.1	114.3	115.7	115.7	115.8	116.0
-O(2'')-	118.9	107.1	113.2	118.9	120.4	121.6	123.2

1. Relative cell volume = 0.80-1.30

In the initial configuration, all the B-O bond lengths were varied in proportion to the cell-volume change. After optimization the intertriangle angles (O-B-O) do not change much, but the connecting angles (B-O-B) change considerably. Thus the shape of the BO₃ triangle does not vary significantly; moreover, the B-O bonds expand by 5%, so that they come close to the uncompressed values. The change in volume is accommodated largely by the change in the B-O-B connecting angles. Among the contributions to the volume change, the change in the B-O bond lengths contributes 28%, while the change in the connecting angles contributes 72%. The change in the B-O-B connecting angles therefore clearly dominates the deformation of the structure.

2. Relative cell volume ~ 0.60

The most interesting result is that the BO_3 triangular structural unit in the minimized structure for the 60% cell volume turns into a BO_4 tetrahedron. This corresponds to a pressure-induced phase transition. Although the original cell is only isotropically compressed and the final structure is not completely the same as B_2O_3 -II, it agrees with the observed phase diagram in that the fourfold BO_4 structural unit is more stable than threefold BO_3 structural unit at high pressure. ¹⁷

In the case of B_2O_3 -II, the structure at 130% volume does not exactly show the reverse structural transformation, but it shows the fourth B-O bond becoming much

longer than the other B-O bonds. Therefore, this suggests that this transformation is probably reversible at 0 K. On the other hand, it is interesting to note that no transformation from B_2O_3 -II to B_2O_3 -I has been ever observed.²² There may be a barrier to the transformation due to entropic factors.

We now consider the manner of the transformation. We note first that the original structures of B_2O_3 -I and B_2O_3 -II are closely related. Considering the latter, if we define the B-O bond length as being shorter than 1.51 Å

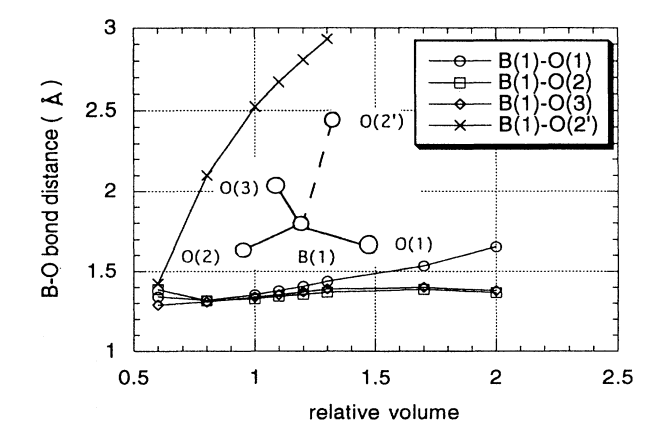
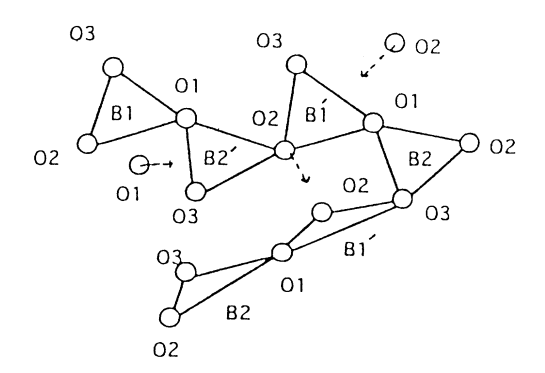


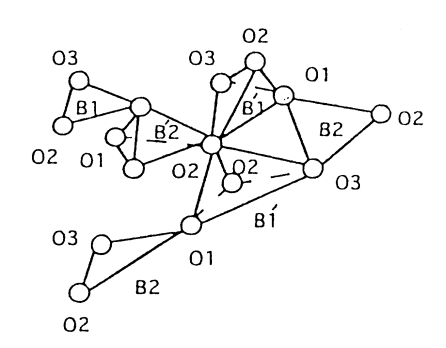
FIG. 4. Relation between the cell volume and B-O bond length in B_2O_3 -I.

then only the first three shortest B-O distances participate in the B-O bonding; all boron atoms become threefold coordinated and all the oxygen atoms become threefold coordinated. These coordination numbers are the same as for B₂O₃-I. Conversely, when B-O bonding is assumed to be within 2.7 Å in B₂O₃-I, that is, the first four shortest B-O distances participate in B-O bonding, all the boron atoms become fourfold coordinate, and one-third of the oxygen atoms become twofold coordinated and the remaining two-third become threefold coordinated. These coordination numbers are the same as for B₂O₃-II. It is interesting that Berger's data, 23,24 for B₂O₃-I which was shown by Strong and Kaplow, 25 and by Gurr et al. 15 to be incorrect, has the same distribution of coordination numbers if the cutoff in the B-O bonding is assumed to be 1.8 Å. Therefore, Berger's data are not far from those of the other two authors, although Berger concluded that B₂O₃-I consists of BO₄ tetrahedra.

With this background we can explain the observed manner of the transformation in B_2O_3 -I as follows: As its cell volume is reduced, the O(1) or O(2) atom approaches the third new boron atom, B(2') or B(1'), which lies on the other ribbon, and the oxygen and boron atoms start to bond. However, the O(3) atom, which cross links the different ribbons of the BO₃ triangle, keeps it coordina-



(a) relative cell volume = 1.0 (BO3 structural unit)



(b) relative cell volume = 0.6 (BO₄ structural unit)

FIG. 5. Schematic diagram for structural transformation.

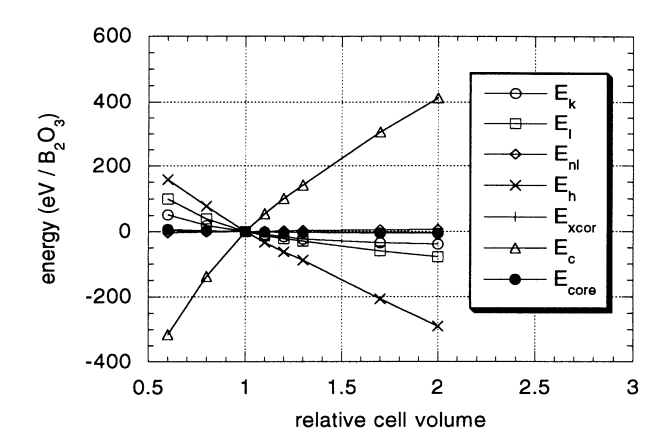


FIG. 6. Various energy contributions to the total energy in B_2O_3 -I. (E_k is the total kinetic energy; E_1 is the local pseudopotential energy; E_{nl} is the nonlocal pseudopotential energy; E_k is the Hartree energy; $E_{\rm excor}$ is the exchange-correlation energy correction; E_c is the Coulombic energy; $E_{\rm core}$ is the core energy.)

tion. The change in the B-O bond distances is shown in Fig. 4. The pattern of the structural transformation is shown in Fig. 5.

The B-O coordination number changes from three to four smoothly without breaking any B-O bonds. It is interesting to note that Tsuneyuki 26 also observed the smooth structural transformation from the SiO_4 tetrahedron into the SiO_6 octahedron in his MD study.

What is the driving force for this transformation? It is useful to analyze the individual energy contributions to the total energy, as was shown by Yin and Cohen. These are shown in Table VIII and Figs. 6 and 7. The contribution of the Coulombic energy (E_c) is much larger than that of the others. When the cell volume is reduced, the Coulombic energy becomes larger, and as is well

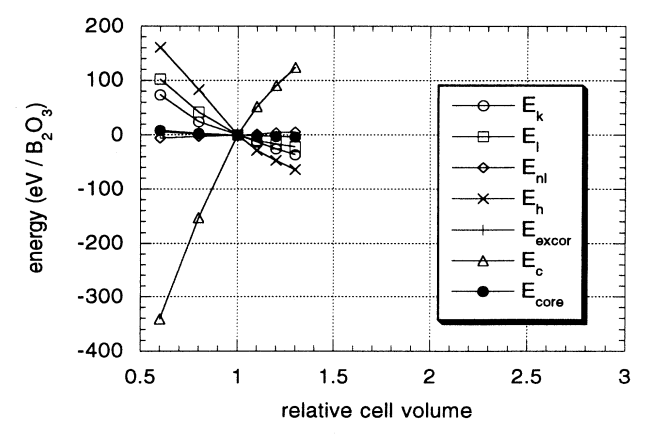


FIG. 7. Various energy contributions to the total energy in B_2O_3 -II. (E_k is the total kinetic energy; E_1 is the local pseudopotential energy; E_{nl} is the nonlocal pseudopotential energy; E_k is the Hartree energy; $E_{\rm excor}$ is the exchange-correlation energy correction; E_c is the Coulombic energy; $E_{\rm core}$ is the core energy.)

TABLE VIII. Comparison of various contributions to the total energy in B₂O₃-I and B₂O₃-II. (Relative cell volume is the ratio to the optimized cell volume.)

\mathbf{B}_2 - \mathbf{O}_3 - \mathbf{I}	(eV/	B_2O_3)					
Volume ratio	0.6	0.8	1.0	1.1	1.2	1.3	1.7
Total kinetic energy	992.94	959.38	940.78	932.50	924.87	917.76	905.87
Local potential energy	-1182.92	-1242.35	-1282.02	-1294.40	-1303.78	-1310.85	-1341.47
Nonlocal potential energy	226.99	229.31	236.65	231.80	233.05	234.28	236.10
Hartree energy	-270.55	-351.10	-428.66	-461.61	-490.83	-516.67	-635.58
Exchange-correlation	110.46	107.72	106.10	105.40	104.75	104.14	103.03
Coulombic energy	-1336.11	-1159.29	-1021.02	-966.76	-920.05	-879.56	-715.43
Pseudopotential core energy	18.51	13.88	11.10	10.09	9.25	8.54	6.53
Total energy	-1440.68	—1442.44	-1443.06	-1442.99	-1442.75	-1442.36	-1440.94
B_2O_3 -II	(e V /]	B_2O_3)					
Volume ratio	0.6	0.8	1.0	1.1	1.2	1.3	
Total kinetic energy	1017.84	969.27	944.14	931.53	918.67	907.69	
Local potential energy	-1128.88	-1188.96	-1231.32	-1241.91	-1247.78	-1253.03	
Nonlocal potential energy	228.27	231.42	233.70	235.52	237.60	239.34	
Hartree energy	-202.41	-280.21	-363.06	-391.71	-410.45	-427.25	
Exchange-correlation	112.77	108.97	106.82	105.78	104.72	103.81	
Coulombic energy	-1488.57	-1300.32	-1147.37	-1094.81	-1056.79	-1023.15	
Pseudopotential core energy	22.89	17.17	13.74	12.49	11.45	10.57	
Total energy	-1438.10	-1442.65	-1443.36	-1443.12	-1442.58	-1441.83	

known this Coulombic energy favors high coordination. On the other hand, when the cell volume increases, the electronic kinetic energy (E_k) , the electron-electron Coulomb energy (E_h) , and nonlocal pseudopotential energy (E_{nl}) are reduced. This favors the lower coordination state in which the valence electrons prefer to be uniformly distributed. The Coulombic contribution is clearly, however, the driving force for the transformation from the B_2O_3 -I to B_2O_3 -II structures.

3. Relative cell volume ≈ 2.0

The 170% cell volume corresponds to the volume in the 1500 K molten state. However, even in the case of 200% cell volume, the structure still keeps the same structural units and the boroxol ring is not observed. It is interesting to note that one of the longest B-O bonds is elongated, while the other two bonds begin to shorten. Although the longest bond is still thought not to be broken, its bonding is weakened and the other two bonds are strengthened. This means that the bonding state is changing from threefold to twofold coordination. This structural feature may be present in the molten state.

The application of first-principles total-energy calculations to B_2O_3 has given the following important results.

- (i) A common set of pseudopotentials for boron and oxygen can reproduce two different crystal structures $(B_2O_3\text{-II})$ well. With this pseudopotential, not only lattice parameters but also internal coordinates are adequately modeled.
- (ii) The bulk modulus is estimated as 26 GPa for B₂O₃-I and 126 GPa for B₂O₃-II.
- (iii) When the cell volume is reduced, the structural transformation from the BO₃ triangular structural unit into the BO₄ tetrahedral unit is observed. The manner of its transformation has also been elucidated.

The CASTEP program can be used for MD. In the near future, the structure of a large system, that is a super cell of a disordered system, will be simulated. At the moment the feasible number of atoms would be 50-60 which when used would be difficult in realistically reproducing the vitreous structure. In subsequent papers, we will, however, show how the structure of glassy B_2O_3 may be modeled using MD simulation methods employing effective potentials.

IV. CONCLUSIONS

¹A. Takada, Ph.D. thesis, University College London, London,

²M. C. Payne, M. P. Teter, D. C. Allan, T. A. Arias, and J. D. Joannopoulos, Rev. Mod. Phys. 64, 1045 (1992).

³R. Car and M. Parrinello, Phys. Rev. Lett. **55**, 2471 (1985).

⁴P. Hohenberg and W. Kohn, Phys. Rev. 136, B864 (1964).

⁵W. Kohn and L. J. Sham, Phys. Rev. 140, A1133 (1965).

⁶E. Wimmer, in *Density Functional Methods in Chemistry*, edited by J. K. Labanowski and W. Andzelm (Springer-Verlag, Berlin, 1991).

⁷J. C. Philips, Phys. Rev. **112**, 685 (1958).

⁸V. Heine, Solid State Phys. 24, 1 (1970).

⁹J. S. Lin, A. Qteish, M. C. Payne, and V. Heine, Phys. Rev. B 47, 4174 (1993).

- ¹⁰M. C. Payne, J. D. Joannopoulos, D. C. Allan, M. P. Teter, and D. H. Vanderbilt, Phys. Rev. Lett. 56, 2656 (1986).
- ¹¹M. J. Gillan, J. Phys. C 1, 689 (1989).
- ¹²M. P. Teter, M. C. Payne, and D. C. Allan, Phys. Rev. B 40, 12 255 (1989).
- ¹³D. J. Chadi and M. L. Cohen, Phys. Rev. B 8, 5747 (1973).
- ¹⁴H. J. Monkhorst and J. D. Pack, Phys. Rev. B 13, 5188 (1976).
- ¹⁵G. E. Gurr, P. W. Mongomery, C. D. Knutson, and B. T. Gorres, Acta Crystallogr. Sec. B 26, 906 (1970).
- ¹⁶C. T. Prewitt and R. D. Shannon, Acta Crystallogr. Sec. B 24, 869 (1968).
- ¹⁷J. D. Mackenzie and W. F. Claussen, J. Am. Ceram. Soc. 44, 79 (1961).
- ¹⁸R. Nada, C. R. A. Catlow, R. Dovesi, and C. Pisani, Phys.

- Chem. Miner. 17, 353 (1990).
- ¹⁹F. D. Murnaghan, Proc. Natl. Acad. Sci. U.S.A. 30, 244 (1944).
- ²⁰M. T. Yin and M. L. Cohen, Phys. Rev. B 26, 5668 (1982).
- ²¹J. P. Poirier, Introduction to the Physics of the Earth's Interior (Cambridge University Press, London, 1991).
- ²²D. R. Uhlmann, J. F. Hays, and D. Turnbull, Phys. Chem. Glasses 8, 1 (1967).
- ²³S. V. Berger, Acta Crystallogr. Sec. **5**, 389 (1952).
- ²⁴S. V. Berger, Acta. Scand. 7, 611 (1953).
- ²⁵S. L. Strong and R. Kaplow, Acta Crystallogr. Sec. B 24, 1032 (1968).
- ²⁶S. Tsuneyuki, in *Molecular Dynamics Simulations*, edited by F. Yonezawa (Springer-Verlag, Berlin, 1992).